



Research Paper

Using *Amaranthus* green proteins as universal biosurfactant and biosorbent for effective enzymatic degradation of diverse lignocellulose residues and efficient multiple trace metals remediation of farming lands

Meysam Madadi^{a,b,1}, Youmei Wang^{a,c,1}, Chengbao Xu^{a,b}, Peng Liu^{a,b}, Yanting Wang^{a,b}, Tao Xia^{a,c}, Yuanyuan Tu^{a,b}, Xinchun Lin^d, Bo Song^e, Xiaoe Yang^f, Wanbin Zhu^g, Deqiang Duanmu^c, Shang-wen Tang^{b,*}, Liangcai Peng^{a,b,**}

^a Biomass & Bioenergy Research Center, College of Plant Science & Technology, Huazhong Agricultural University, Wuhan 430070, China

^b Laboratory of Biomass Engineering & Nanomaterial Application in Automobiles, College of Food Science & Chemical Engineering, Hubei University of Arts & Science, Xiangyang, China

^c College of Life Science & Technology, Huazhong Agricultural University, Wuhan 430070, China

^d State Key Lab Subtrop Silviculture, College of Forestry & Biotechnology, Zhejiang Agricultural & Forestry University, Hangzhou 311300, Zhejiang, China

^e College of Environmental Science & Engineering, Guilin University of Technology, Guangxi, China

^f College of Environmental & Resource Sciences, Zhejiang University, Hangzhou 310058, Zhejiang, China

^g College of Agronomy & Biotechnology, China Agricultural University, Beijing 100193, China



ARTICLE INFO

Editor: Dr. A. Daugulis

Keywords:

Amaranth proteins
Biosurfactant
Green-like process
Biomass saccharification
Trace-metal remediation

ABSTRACT

Improving biomass enzymatic saccharification is effective for crop straw utilization, whereas phytoremediation is efficient for trace metal elimination from polluted agricultural soil. Here, we found that the green proteins extracted from *Amaranthus* leaf tissue could act as active biosurfactant to remarkably enhance lignocellulose enzymatic saccharification for high bioethanol production examined in eight grassy and woody plants after mild chemical and green-like pretreatments were performed. Notably, this study estimated that total green proteins supply collected from one-hectare-land *Amaranth* plants could even lead to additional 6400–12,400 tons of bioethanol, being over 10-fold bioethanol yield higher than those of soybean seed proteins and chemical surfactant. Meanwhile, the *Amaranth* green proteins were characterized as a dominated biosorbent for multiple trace metals (Cd, Pb, As) adsorption, being 2.9–6 folds higher than those of its lignocellulose. The *Amaranth* plants were also assessed to accumulate much more trace metals than all other plants as previously examined from large-scale contaminated soils. Furthermore, the *Amaranth* green proteins not only effectively block lignin to release active cellulases for the mostly enhanced biomass hydrolyzes, but also efficiently involve in multiple chemical bindings with Cd, which should thus address critical issues of high-costly biomass waste utilization and low-efficient trace metal remediation.

1. Introduction

By photosynthesis, plants are capable to convert solar energy into biomass substances, providing protein, starch and lignocellulose residues. However, although lignocellulose residues cover more than half of

total plant biomass particularly in crop straws, large amounts of lignocellulose residues are not well utilized, leading to as the wastes remaining in farming lands and human life locations (Ragauskas et al., 2006; Sun et al., 2016). Over the past years, attempts have been made to convert the lignocellulose into biofuels and bioproducts, and in

Abbreviations: AP, *Amaranth* proteins; SP, soybean proteins; Cd, cadmium; Pb, lead; As, arsenic; BSA, bovine serum albumin; LHW, liquid hot water; SE, steam explosion; CaO, calcium oxide; NaOH, sodium hydroxide; CBH-I, exo- β -1,4-D-glucanase.

* Corresponding author.

** Corresponding author at: Biomass & Bioenergy Research Center, College of Plant Science & Technology, Huazhong Agricultural University, Wuhan 430070, China.

E-mail addresses: tsw830629@163.com (S.-w. Tang), lpeng@mail.hzau.edu.cn (L. Peng).

¹ These authors contributed equally.

<https://doi.org/10.1016/j.jhazmat.2020.124727>

Received 23 August 2020; Received in revised form 17 October 2020; Accepted 27 November 2020

Available online 1 December 2020

0304-3894/© 2020 Elsevier B.V. All rights reserved.

particular, cellulosic bioethanol has been defined as the promising second generation of biofuel for reduced net carbon emission (De Souza et al., 2014; Kim et al., 2020; Yang et al., 2018). Nevertheless, as lignocellulose recalcitrance basically causes an unacceptably costly bioethanol conversion along with unavoidable secondary wastes release into the environment (Chen et al., 2016; Demartini et al., 2013), it becomes essential to find out a cost-effective and green-processing technology for complete utilization of crop lignocellulose residues.

Lignocellulose recalcitrance is fundamentally determined by plant cell wall composition, wall polymer feature, and wall-network style (Wang et al., 2016). Although various biomass pretreatments under extreme conditions are effective to break down lignocellulose recalcitrance (Baruah et al., 2018; Liu et al., 2019), the most techniques simply cause a costly biomass process and produce numerous toxic compounds that affect sequential enzymatic hydrolysis and inhibit final yeast fermentation (Dos Santos et al., 2019; Shinde et al., 2018). Exceptionally, liquid hot water, steam explosion, and CaO pretreatments have been applied as environment-friendly technology to enhance biomass enzymatic saccharification (Alam et al., 2019; Sun et al., 2017; Wu et al., 2019a; Zahoor et al., 2017). Because the biomass residues are of diverse lignocellulose compositions and features among different crop species, it also remains to explore a universal strategy applicable for all types of biomass resources.

Chemical surfactants especially non-ionic chemicals have been applied to enhance lignocellulose enzymatic saccharification (Wang et al., 2018). For instance, Tween-80 could specifically block cellulase adsorption for largely enhanced enzymatic hydrolysis and bioethanol conversion in common reed (Jin et al., 2016). Meanwhile, bovine serum albumin (BSA) and soybean seed protein are also examined to play a surfactant-like role for enhancing biomass enzymatic hydrolysis (Wei and Wu, 2017; Florencio et al., 2016). However, the supplements with chemical surfactants, BSA, and soybean proteins still cause overpriced enzymatic hydrolysis of biomass residues at large scale, and particularly the soybean proteins supply could not avoid the conflict with food and feed security (Liu et al., 2018). Furthermore, much is unknown about mechanism of how surfactants could improve biomass enzymatic hydrolysis while various physical and chemical pretreatments are performed with diverse lignocellulose resources (Zhou et al., 2015). Hence, it should be more important to identify the non-chemical surfactant that is of low cost and high activity for enhancing biomass enzymatic saccharification at large scale.

Cadmium (Cd), lead (Pb) and arsenic (As) are the major trace metals that are of toxicity to human beings and animals, and they have been examined to contaminate agricultural lands and daily life locations over the world (Peng et al., 2009; Vardhan et al., 2019). Since special plant species could accumulate individual trace metals, plant phytoremediation has been regarded as a green-like biotechnology for trace metal elimination (Cheng et al., 2019, 2018). For large scale phytoremediation, however, it is important to sort out what is the major compound strongly associated with trace metals in the lignocellulose-rich biomass residues.

Amaranthus retroflexus L. is a fast-growing C4 grass consisting of 60–70 species for wide-ranging ecological adaptability, and thus it can grow up to 1.5–3 m height for enormous biomass resource with relatively less requirements of water and fertilizer supplies (Jonathan, 1986). Particularly, the *Amaranthus* plant is of rich proteins ranged from 10% to 38% in the green tissues such as leaves and stems, and those green proteins have thus been considered as nutrition additive into food and feed (Grobelnik Mlakar et al., 2010). As the *Amaranthus* plant produces large amounts of green proteins, it would be interesting to test their roles in biomass enzymatic hydrolysis and trace metal phytoremediation. In this study, we extracted the most proteins from the *Amaranthus* fresh leaves and then co-supplied into enzymatic hydrolyses of diverse lignocellulose substrates. By comparison with classic chemical surfactant (Tween-80) and soybean seed proteins, this study detected that the *Amaranth* proteins at less dosage supply could even enhance

more biomass enzymatic saccharification for extra bioethanol production under mild-chemical and green-like pretreatments performed in eight representative grassy crops and woody trees. Meanwhile, we determined that the *Amaranth* proteins accumulated large amounts of three trace metals (Cd, Pb, As) *in vivo* and *in vitro*, indicating that the *Amaranth* proteins should play a dominated biosorbent role in plant phytoremediation. Furthermore, this study in-depth performed chemical and biochemical integrated analyses to sort out mechanisms of how the *Amaranth* proteins could either play an universal biosurfactant role for enhanced lignocellulose enzymatic saccharification of all major crops and trees or act as a dominated biosorbent for trace metals remediation, thereby providing a cost-effective and green-process strategy to enhance biomass degradation for cellulosic ethanol productivity or to remove multiple trace metals from polluted agricultural lands at large scale.

2. Material and methods

2.1. Collection of biomass samples

Seven types of biomass samples of grassy crops (rice, wheat, rapeseed, *Miscanthus*, and corn) and woody trees (poplar and *Eucalyptus*) were respectively collected from Huazhong Agricultural University experimental station. All biomass samples and stem tissues of *Amaranth* plant (*Amaranthus retroflexus* L. provided by China *Amaranth* Ecological Technology Co., Ltd.) were dried at 50 °C until constant weight, ground through a 40-mesh screen and stored in the sealed container until use.

2.2. Wall polymer extraction and determination

Plant cell wall fractionation procedure was performed as previously described by Peng et al. (2000) with minor modification in this study. The soluble sugars, lipid, starch, and pectin of biomass samples were consecutively extracted by using potassium phosphate buffer (pH 7.0), chloroform-methanol (1:1, v/v), DMSO-water (9:1, v/v) and ammonium oxalate 0.5% (w/v). The remaining crude residues were extracted with 4 M KOH with 1.0 mg/mL sodium borohydride for 1 h at 25 °C and the combined supernatants were used as KOH-extractable hemicelluloses fraction. The remaining pellets were applied to detect total hexoses for cellulose level by the anthrone/H₂SO₄ method (Fry, 2000). Total hemicelluloses level was calculated by detecting pentoses of the non-KOH-extractable pellets by the orcinol/HCl method (Dische et al., 1962) and total hexoses and pentoses in the KOH-extractable fraction. Total lignin consisting of acid-soluble and insoluble lignin was measured using the Laboratory Analytical Procedure of the National Renewable Energy Laboratory (Sluiter et al., 2008). All analyses were performed in independent triplicate.

To detect monosaccharide composition of hemicelluloses fraction, GC-MS (SHIMADZU GCMS-QP2010 Plus) method was applied as previously described by Li et al. (2015). Trifluoroacetic acid (TFA) and *myo*-inositol were obtained from Aladdin Reagent Inc. 1-Methylimidazole was purchased from Sigma-Aldrich Co. LLC. Acetic anhydride and acetic acid were obtained from Sinopharm Chemical Reagent Co., Ltd.

2.3. Plant protein extraction

The well-dried *Amaranth* green tissues and soybean seeds (purchased from commercial market) were respectively ground twice into powders with liquid nitrogen, and the pestle and mortar were rinsed with 10 mL buffer (0.2 M Na-acetate, pH 4.5). The combined homogenates were transferred into 15 mL plastic tubes, shaken under 150 rpm at 25 °C for 30 min and centrifuged at 3000 × g for 5 min. All supernatants were collected as the extractable protein samples for the following experiments.

2.4. Amino acids assays and protein Western blot analysis

The extracted proteins from *Amaranth* and soybean samples were determined by Nitrogen Analyzer (SpectraMax i3x Multi-Mode Detection Platform, USA) as previously described by Da Silva et al. (2016) with minor modification in this study. A total of 0.2 g protein samples was suspended with 4 g solution ($\text{CuSO}_4 + \text{K}_2\text{SO}_4$, 1:8), added with 12 mL (v/v) H_2SO_4 , and heated at 320 °C for 3 h until completely oxidized. After tubes were cooled down, the samples were added with distilled water up to 100 mL and 300 μL of filtrated samples were used for total nitrogen assay. The crude protein was calculated by converting total nitrogen into protein-beyond 6.25 according to Eq. (1) as previously described by Mariotti et al. (2008).

$$\text{Crude protein}(\%) = (A \times D) \times 100/W \times 6.26 \quad (1)$$

where A; the absorbance of samples by Nitrogen Analyzer; D: sample dilution with distilled water; W: the weight (g) of samples.

An Automatic Amino Acid Analyzer (L-8900 Tokyo, Japan) was applied to determine amino acid compositions of proteins samples as previously described by Andini et al. (2013). Total 0.2 g dried samples with 10 mL 6 N HCl were added into the cylinder glass tubes and oxidized under cold vacuum condition. The vacuum-sealed glass tube was heated at 110 °C for 24 h, and then the vacuum-dried hydrolysates were added with distilled water. After centrifugation for 10 min at 3000 \times g, the supernatants were transferred into an Erlenmeyer flask through a 0.45 μL nylon membrane filter with the pipette. A rotary evaporator was used to remove HCl in the solution. After the solution is dried up, 5 mL sodium acetate buffer was added and then filtered through a 0.22 μL nylon membrane filter. About 300 μL filtrate was used to measure amino acids. The experiments were conducted in independent triplicates.

For Western blot analysis, the protein samples were loaded into 12% SDS-PAGE gel, and Western blot analysis was performed as previously described by Li et al. (2017).

2.5. Physical and chemical pretreatments of biomass residues

All physical and chemical pretreatments were performed as previously described including steam explosion (SE), liquid hot water (LHW), lime (CaO), and alkali (NaOH) pretreatments (Alam et al., 2019; Wu et al., 2019a; Zahoor et al., 2017). The control samples (without pretreatments) were added with distilled water and shaken for 2 h at 50 °C. All samples were conducted in independent triplicate.

SE pretreatment: The well-dried wheat, rapeseed, *Miscanthus*, and corn straw samples (200 g) were respectively loaded with Steam Explosion Reactor (QBS-200, Hebi Zhengdao Machine Factory, Hebi, China) using previously-established condition (2.5 MPa, 200 °C, 3 min (Zahoor et al., 2017)). The steam-exploded residues were dried and ground into powders through a 40-mesh screen and stored for further experiments.

LHW pretreatment: The well-mixed *Amaranth* and rice biomass samples were respectively suspended with 2.4 mL distilled water in a well-sealed Teflon gasket with stainless steel bombs, and heated at 200 °C under 15 rpm for 2, 4, 8, 16, and 32 min. The sealed bombs were directly cooled down and the liquors were transferred into 15 mL plastic centrifuge tubes with distilled water into the final volume up to 6 mL. The tubes were further centrifuged at 3000 \times g for 5 min and the supernatant was used for determination of total pentoses and hexoses.

CaO pretreatment: The well-dried *Amaranth* and rice biomass samples were respectively added into 6 mL CaO at various concentrations (1%, 2.5%, 5%, 10%, 15% w/w) for 48 h at 50 °C. The samples were neutralized with 10% HCl or H_2SO_4 , centrifuged for 5 min at 3000 \times g, and washed with distilled water for 5–6 times until pH 7. All supernatants were collected for determination of pentoses and hexoses.

NaOH pretreatment: The well-mixed poplar and *Eucalyptus* biomass

samples were respectively added with 6 mL solution of NaOH at different concentrations (1%, 2%, 4%, 8%, 12% w/v) and shaken under 150 rpm at 50 °C for 2 h. After centrifugation at 3000 \times g for 5 min, all supernatants were collected for pentoses and hexoses assay.

For LHW, CaO, and NaOH pretreatments, the remained residues were washed with distilled water for at least 5 times until pH 7, and then rinsed once with 0.2 M Na-acetate buffer (pH 4.8) for the sequential enzymatic hydrolysis as described below.

2.6. Biomass enzymatic hydrolysis co-supplied with surfactant and protein

Enzymatic hydrolysis with 5% biomass loading was performed as previously described by Li et al. (2018) with minor modification in this study. The remaining residues from pretreatments were washed with 0.2 M Na-acetate buffer (pH 4.8), and incubated with 2 g L^{-1} (w/v) mixed-cellulases including the final concentrations of cellulases at 10.60 FPU g^{-1} biomass and xylanase at 6.72 U g^{-1} biomass, while co-supplied with/without various concentration of *Amaranth* proteins and soybean proteins (2%, 4%, 8%, 12%, 16%; w/w) or Tween-80 (0.6%, 0.8%, 1%, 1.6%, 2%; v/v). In addition, the pretreated residues of rice (LHW) and corn (SE) were incubated with the commercial cellulases enzymes (Cellic CTec2) at a dosage of 113.3 FPU/mL. Filter paper assay was used to measure mixed-cellulases activity based on the International Union of Pure and Applied Chemistry (IUPAC) guidelines, 1 FPU = 1 $\mu\text{mol min}^{-1}$ of “glucose” (reducing sugars as glucose). The xylanase activity was determined by using commercial 1% (w/v) xylan (Sigma-Aldrich Co. LLC, California, USA) as substrate, 1 U = 1 $\mu\text{mol min}^{-1}$ of “xylose”. The hydrolysis reactions were performed under 150 rpm at 50 °C for 48 h. After centrifugation at 3000 \times g for 5 min, the supernatants were collected to determine total pentoses and hexoses yields released from enzymatic hydrolysis according to Eq. (2):

$$\text{Hexoses yield}(\%) = \text{Hexoses released}(\text{g}) \times 100/\text{Cellulose content}(\text{g}) \quad (2)$$

where hexoses released (g) from substrates after 48 h enzymatic hydrolysis; cellulose content (g) of the raw substrates presented in Table S2. All experiments were carried out in independent triplicate.

2.7. Yeast fermentation and ethanol assay

Yeast fermentation was conducted using total hexoses released from both pretreatment and sequential enzymatic hydrolysis as previously described by Jin et al. (2016). *Saccharomyces cerevisiae* strain (purchased from Angel yeast Co., Ltd., Yichang, China) was used in all fermentation reactions. The ethanol yield was estimated using $\text{K}_2\text{Cr}_2\text{O}_7$ method as described by Hu et al. (2018). Absolute ethanol (99.9%) was used as the standard. The sugar-ethanol conversion rate (%) was calculated according to Eq. (3):

$$S - E(\%) = E/(F \times H) \times 100 \quad (3)$$

where S-E: sugar-ethanol conversion rate (%); E: total ethanol weight (g) at the end of fermentation; F: the theoretical conversion rate at 0.511 (92/180) in the case when glucose is entirely fermented to ethanol according to the Embden–Meyerhof–Parnas pathway in *S. cerevisiae*; and H: total hexoses weight (g) at the beginning of fermentation (released from both pretreatment and enzymatic hydrolysis). The fermentation experiments were conducted in independent triplicate.

2.8. Proteins binding assay

Protein binding assay was conducted as previously described by Henshaw et al. (2004) with minor modification in this study. About 5 mg *Amaranth* proteins (per mL) was incubated in 0.2 M Na-acetate buffer (total volume of 10 mL, pH 4.8) with the lignin residues

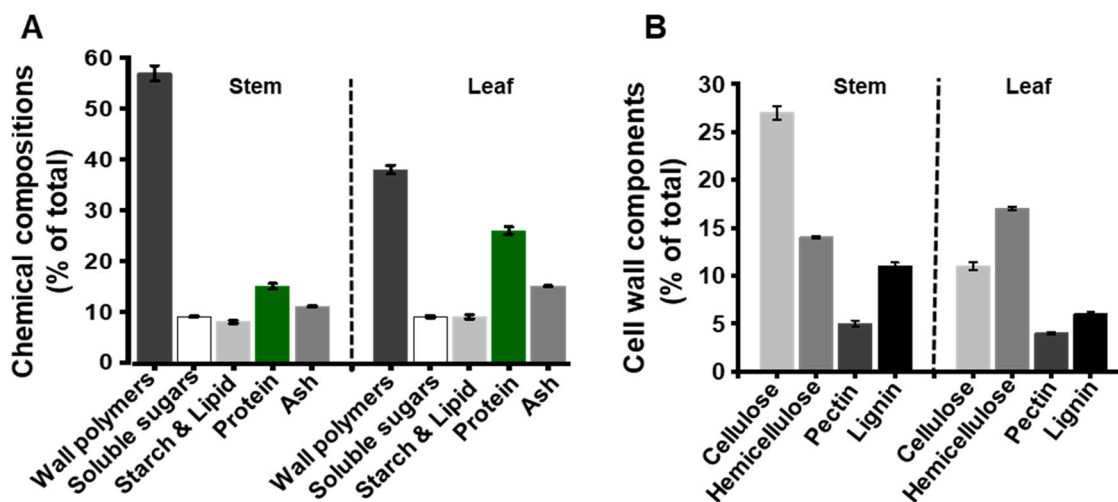


Fig. 1. Lignocellulose compositions of mature *Amaranthus retroflexus* L. straw. (A) All compounds of stem and leaf tissues (% of total). (B) Wall polymer proportions of stem and leaf tissues (% of total). Data as means \pm SD ($n = 3$).

prepared from rice material in this study and the commercial standard samples including lignin, xylan, and avicel. After shaken at 25 °C for 4 h, the samples were centrifuged at 4000 \times g for 5 min to collect unbound proteins in supernatants, and the Bradford assay was applied to detect the proteins content. The bound proteins were calculated by subtracting the amount of unbound proteins from total proteins. All experiments were performed at independent triplicate.

2.9. Measurement of zeta potential and surface tension

Zeta potential of lignin microparticles in biomass samples was analyzed by a Dynamic Light Scattering (DLS) Analyzer equipped with a laser Doppler microelectrophoresis (Zetasizer Nano ZS90, Malvern Instruments, Malvern, UK) as previously described by Luo et al. (2019). The samples were filtered by 0.45 μ m syringe membranes (Millipore, Billerica, MA, USA) for analysis and deionized water was used for background correction. Zeta potential measurements were performed in independent triplicate.

Surface tension measurements were performed by the Wilhelmy plate method using a NIMA ST-9000 tensiometer (Nima Technology, Coventry, UK) as previously described by Zhu et al. (2019). A platinum plate (10.04 \times 0.15 mm) supplied by Nima Technology was used for all surface tension measurements. The plate was cleaned with 75% ethanol and distilled water and then flamed before each measurement. Each sample was measured for equilibrium surface tension after at least 10 min to ensure the saturation of surfactant adsorption on the air/water interface. The tensiometer was calibrated as per the operating instructions and the surface tension of Milli-Q water was measured to ensure accuracy. The surface tension of the *Amaranth* solution was measured immediately and maintained at an ambient temperature of approximately 23 °C.

2.10. Trace metals detection

Trace metal levels of various biomass protein samples were determined as previously described by Cheng et al. (2019) and Zhou et al. (2017). For the extracted protein samples as described above, 70% ethanol was used to remove soluble sugars in the supernatant and the soluble trace metals were vacuum-dried for 72 h at 25 °C. The well-dried samples were digested with HNO₃ and then an automatic absorption spectrometer (Agilent 240Z GFAA) was applied to detect Cd and Pb levels. The well-mixed powder was aqua-regia digitized with HNO₃/H₂SO₄/HClO₄ and an atomic fluorescence spectrometer (AFS-8220, Titan Instruments) was applied to detect As level. All

experiments were carried out in independent triplicate.

2.11. Cd adsorption assay

Both extractable *Amaranth* proteins and lignocellulose residue samples were respectively dried at 50 °C under air oven for Cd adsorption assay. Solutions of Cd was prepared by adding Cd (NO₃)₂ into ultra-pure water at room temperature. Batch adsorption experiments were performed for 4 h in 50 mL tubes at 150 rpm as previously described by Xu et al. (2020) and Zhang et al. (2020). Biosorption experiments were performed under the operating condition: pH (4.0–8.0), initial metal concentration (10–100 mg/L) and protein with or without DNase enzyme. The samples were filtered through a 3 KD ultrafiltration tube and the residual Cd in the filtrate was determined by flame atomic absorption spectrophotometer (FAAS HITACHI Z-2000, Japan) equipped with air-acetylene flame. The amount of adsorption at equilibrium q_e (mg g⁻¹) and the percentage removal efficiency (%R) were calculated as previously described by Yu et al. (2008). The biosorbents were also characterized using X-ray photoelectron spectroscopy (XPS, Escalab 250Xi, Thermo Fisher, USA) (Yu et al., 2015). All assays were conducted in independent triplicate.

2.12. Statistical analysis of correlation coefficients

Superior Performance Software Systems (SPSS version 17.0, Inc., Chicago, IL) was applied for statistical analysis. Correlation coefficients were determined using Spearman's rank for all measured parameters. Pair-wise comparisons were conducted between two measurements by Student's *t*-test. Means were separated by the least significant difference (LSD) test at $P < 0.05$. The line graph for the best fit curve was generated using Origin 8.5 software (Microcal Software, Northampton, MA). The average values were calculated from the original triplicated measurements for these analyses.

3. Results and discussion

3.1. *Amaranth* plants are rich at high quality of lignocellulose and proteins

Although *Amaranthus retroflexus* L. is the typical C4 grassy plant consisting of 60–70 species for diverse ecological distributions (Jonathan, 1986), much remains unknown about its biomass yield and protein constitution. By referring with the worldwide data (Akond et al., 2013; Vıglasky et al., 2009), this study respectively measured the fresh and dry

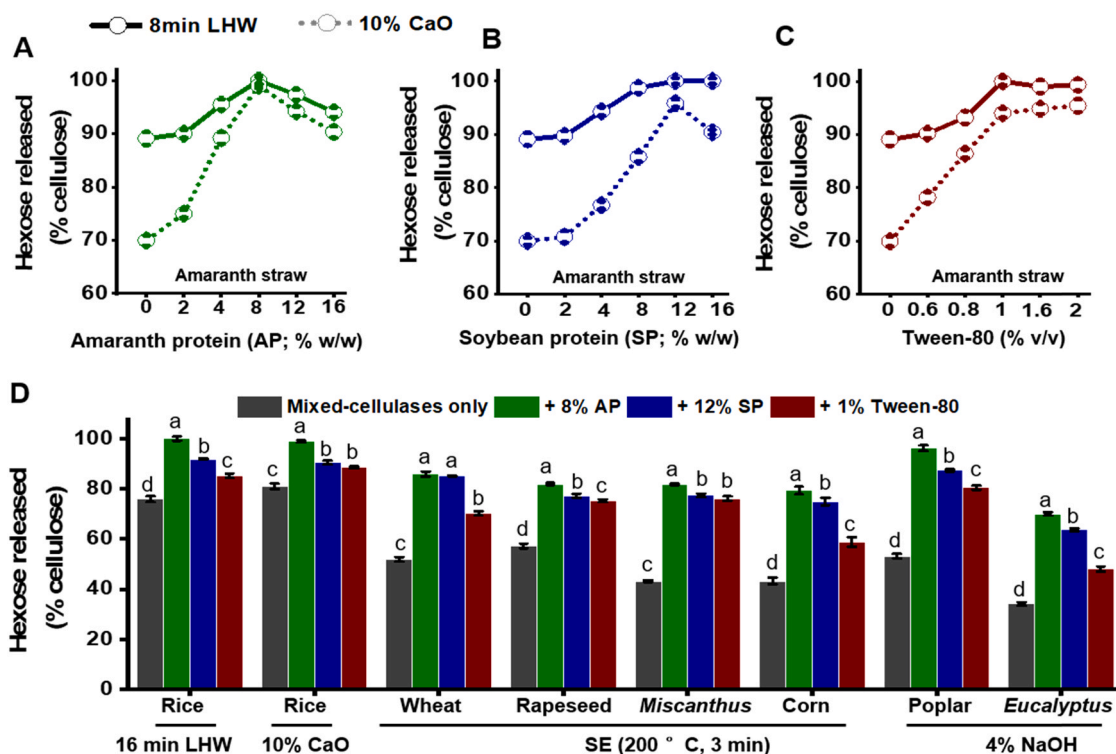


Fig. 2. Biomass enzymatic saccharification under various physical and chemical pretreatments performed in eight crops and trees co-supplied with *Amaranth* proteins (AP), soybean seed proteins (SP), and Tween-80, respectively. (A, B, C) Hexoses yields (% cellulose) released from enzymatic hydrolysis of *Amaranth* straw under liquid hot water (LHW) pretreatment for 8 min and 10% CaO pretreatment co-supplied with AP or SP at series of dosages or Tween-80 at different concentrations. (D) Hexoses yields in seven bioenergy crops co-supplied with optimal surfactants under different physical (LHW, steam explosion/SE) and chemical (CaO, NaOH) pretreatments as previously established (Alam et al., 2019; Wu et al., 2019a; Zahoor et al., 2017). Data as means \pm SD ($n = 3$); Small letters (a, b, c, d) as multiple significant difference by LSD-test at $P < 0.05$.

weights of the *Amaranth* plants ranged from 105 to 225 t/ha and 37–54 t/ha, with the lowest and highest proteins levels between 10.4 and 18.9 t/ha. Using the green tissue samples of *Amaranth* plants collected in this experiment, we determined that lignocelluloses (total wall polymers) cover 57% and 38% (% of total dry weight) of biomass materials in stem and leaf tissues, respectively (Fig. 1A). Notably, both stem and leaf tissues contained much high proteins levels at 15% and 26% (of total), confirming that the *Amaranth* plant was extremely rich at proteins in the green tissues. Meanwhile, this study detected much high soluble sugars (9%) in the green tissues, which would be directly applicable for yeast fermentation to produce additional bioethanol.

Furthermore, this study examined three major wall polymers levels of dry *Amaranth* stem tissues including 27% cellulose (% of total), 14% hemicellulose, 11% lignin, and 5% pectin (Fig. 1B), indicating that the cellulose-rich stem tissue should be the desirable biomass residue for cellulosic ethanol productivity. By comparison, the dry leaf tissue contained much less lignocellulose than that of the stem, due to relatively more proteins and ash. As *Amaranth* leaf tissue contained much high proteins level, this study further detected its amino acid composition (Table S1). Among total of 17 amino acids examined, we examined eight human-essential amino acids covering 45% of the total, which were much higher than those of soybean seed and other cereal grains (Carrera et al., 2011; Gorinstein et al., 2002). Furthermore, this study found that most proteins (84% of total) were extractable from the *Amaranth* leaf tissue, and the extractable proteins contained the highest proportions of two amino acids (Asp and Glu) with relatively high levels of Lys and Arg (Table S1). Because those four amino acids are of distinctively negative and positive charges, it would be interesting to test those extractable proteins roles in biomass enzymatic hydrolysis and trace metal accumulation in the following experiments.

3.2. *Amaranth* proteins are mostly efficient for enhancing biomass enzymatic saccharification in eight major crops and trees

Using previously-established approaches (Alam et al., 2019; Hu et al., 2018; Wu et al., 2019a), this study compared *Amaranth* proteins (AP), soybean proteins (SP) and Tween-80 enhancements on biomass saccharification by measuring hexoses yields (% cellulose) released from enzymatic hydrolyses of pretreated lignocellulose substrates in eight major crops and trees (Fig. 2). Because the *Amaranth* straw is of much high biomass yield as described above, we first detected its biomass saccharification under two green-like pretreatments (8 min liquid hot water/LHW at 200 °C and 10% CaO at 50 °C) as previously established (Alam et al., 2019; Wu et al., 2019a), while co-supplied with *Amaranth* proteins, soybean seed proteins, and Tween-80 at series of concentrations into the enzymatic hydrolysis reactions (Fig. 2A–C). As a result, the supplement with 8% *Amaranth* proteins could lead to almost complete biomass enzymatic saccharification of *Amaranth* straw with hexoses yields of 100% (% cellulose) under two green-like pretreatments performed (Fig. 2A), whereas the controls without *Amaranth* proteins supply only showed the hexoses yields of 89% and 70% (% cellulose), suggesting that the *Amaranth* proteins may play a surfactant-like enhancement role in biomass enzymatic hydrolysis. By comparison, the supplement with a higher dosage of soybean seed proteins (12%) could also cause complete saccharification of *Amaranth* straw under the 8 min LHW pretreatment, but it led to hexoses yield of 95% (%cellulose) under the 10% CaO pretreatment (Fig. 2B). Even though under the higher dosage of soybean proteins (16%) supply, the hexoses yield turned to be a reducing trend, which was consistent with the previous reports that the commercial soybean proteins at high dosage (more than 12%) could not further improve enzymatic hydrolysis of steam-exploded sugarcane bagasse (Brondi et al., 2019; Florencio et al., 2016). Similarly,

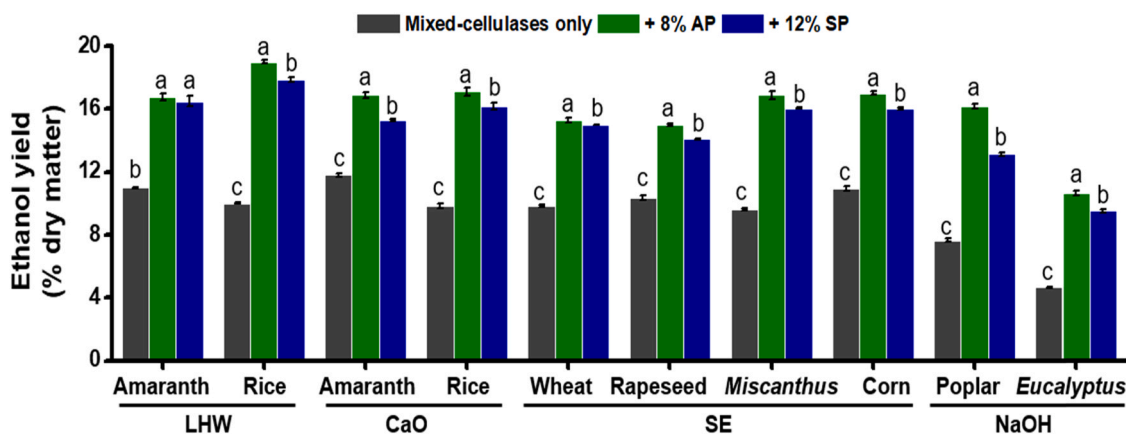


Fig. 3. Bioethanol yields (% dry matter) obtained from yeast fermentation. Ethanol yield achieved in eight crops and trees using total hexoses released from both pretreatment and enzymatic hydrolysis of four optimal pretreatments co-supplied with AP and SP. Data as means \pm SD ($n = 3$), Small letters (a, b, c) as multiple significant difference by LSD-test at $P < 0.05$.

the Tween-80 supplement at the optimal concentration (1%) led to the hexoses yield of 94% under the 10% CaO pretreatment (Fig. 2C). Hence, even though at relatively less dosage supply, the *Amaranth* proteins could exhibit more enhancement for biomass enzymatic saccharification compared to the soybean proteins and Tween-80.

Furthermore, this study selected seven representative grassy crops such as three major food crops (rice, wheat, rapeseed), two C4 bioenergy plants (*Miscanthus*, corn) and two woody trees (poplar, *Eucalyptus*), with distinct cell wall compositions and wall polymer features (Table S2). Using three green-like pretreatments (liquid hot water/LHW, steam explosion/SE, CaO) and one mild alkali pretreatment (NaOH) at their optimal conditions as previously established (Alam et al., 2019; Wu et al., 2019a; Zahoor et al., 2017), this study examined biomass enzymatic saccharification co-supplied with three surfactants (Fig. 2D). In general, the 8% *Amaranth* proteins supplement remained the most enhanced biomass enzymatic saccharification in all seven crops, as compared to the 12% soybean proteins and 1% Tween-80 supplies, consistent with the findings of *Amaranth* straw. Moreover, the supplements of 8% *Amaranth* proteins could even lead to the hexoses yields ranged from 1.44 to 9.40 (g/L) in eight bioenergy crops and trees examined (Fig. S1). In particular, both *Amaranth* and soybean proteins were of significantly higher enhancement capacity on biomass saccharification than those of the Tween-80 at $P < 0.05$ or 0.01 level ($n = 3$) in almost all lignocellulose substrates examined. Provided that the Tween-80 has been examined as a powerful chemical surfactant (Jin et al., 2016), the results obtained in this study suggest that the green proteins should be more effective for enhancing enzymatic saccharification of diverse lignocellulose substrates. In addition, except for the wheat straw, other six crops showed significantly higher hexoses yields released from enzymatic hydrolyzes while co-supplied with the 8% *Amaranth* proteins, compared to the 12% soybean proteins, which confirmed that the *Amaranth* proteins should be of more efficient enhancements for the enzymatic saccharification of diverse lignocellulose residues.

To test the specificity of *Amaranth* proteins, this study co-supplied protein inhibitors and DNases into the biomass enzymatic hydrolysis reactions, respectively (Fig. S2A). Using the pretreated biomass residues of rice and corn straws, we found that co-supplement with proteinase inhibitors or DNases did not significantly affect the *Amaranth* proteins enhancements, suggesting that the *Amaranth* proteins should be stable for saccharification enhancement and the nucleic acids co-extracted with the *Amaranth* proteins may have little impact on biomass enzymatic hydrolysis. Meanwhile, while another commercial cellulases (Cellic CTec2) were applied for biomass enzymatic hydrolysis, the *Amaranth* proteins supply showed the enhancement rate of biomass saccharification similar to the mixed-cellulases examined above

(Fig. S2B). In addition, this study detected the hexoses yields released from enzymatic hydrolysis contain 97–98% glucose and the small proportion of galactose and mannose from the *Amaranth* proteins supply, and the glucose proportions were higher than those of the soybean proteins and Tween-80 supplies (Table S3), suggesting that the *Amaranth* proteins supply should remain more effective for enzymatic hydrolysis of cellulose microfibrils. Thereby, the results indicated that the *Amaranth* proteins are specifically stable and durable for enhancing enzymatic saccharification of diverse lignocellulose residues in eight major crops and trees.

3.3. Bioethanol yields are remarkably elevated in all types of lignocellulose residues upon *Amaranth* proteins supply

As the *Amaranth* proteins play a universal enhancement role in biomass enzymatic saccharification of all eight types of lignocellulose residues examined, this study consequently performed yeast fermentation to measure bioethanol yields (Fig. 3). Compared to the controls (without *Amaranth* or soybean proteins) of eight lignocellulose residues under the four pretreatments performed above, both 8% *Amaranth* proteins and 12% soybean proteins supplements led to significantly increased bioethanol yields, with the elevated rates ranged from 43% to 128% (*Amaranth* proteins) and 30–104% (soybean proteins), respectively (Fig. 3), which are consistent with their distinctively raised hexoses yields (Fig. 2). Among the pretreated biomass samples of eight crops and trees examined, the 8% *Amaranth* proteins supply remained significantly higher bioethanol yields than those of the 12% soybean proteins at $P < 0.01$ levels ($n = 3$).

Based on the hexoses and bioethanol yields obtained in all biomass samples, this study further calculated sugar-ethanol conversion rates (Fig. S3A). By comparison, the 8% *Amaranth* proteins and 12% soybean supplements respectively led to the sugar-ethanol conversion rates at 98% and 94%, whereas the controls had the conversion rate of 84% on the average, suggesting that both green proteins supplies should largely improve yeast fermentation efficiency, probably by either producing less toxic compounds that inhibit yeast fermentation during biomass enzymatic hydrolysis or blocking the toxic compounds with yeast cells (Deng et al., 2020; Sun et al., 2020). Despite that Tween-80 has reportedly improved yeast fermentation (Jin et al., 2016), this study revealed that the green proteins should be of better performance in particular from the *Amaranth* proteins.

By means of the collected data of maximum dry biomass yields per year of eight major crops in the farming fields (Table S4), this study in theory evaluated the potential bioethanol yields at large scale, subjective to their biomass enzymatic saccharification and sugar-ethanol conversion rates obtained above (Fig. S3B). Due to the highest dry

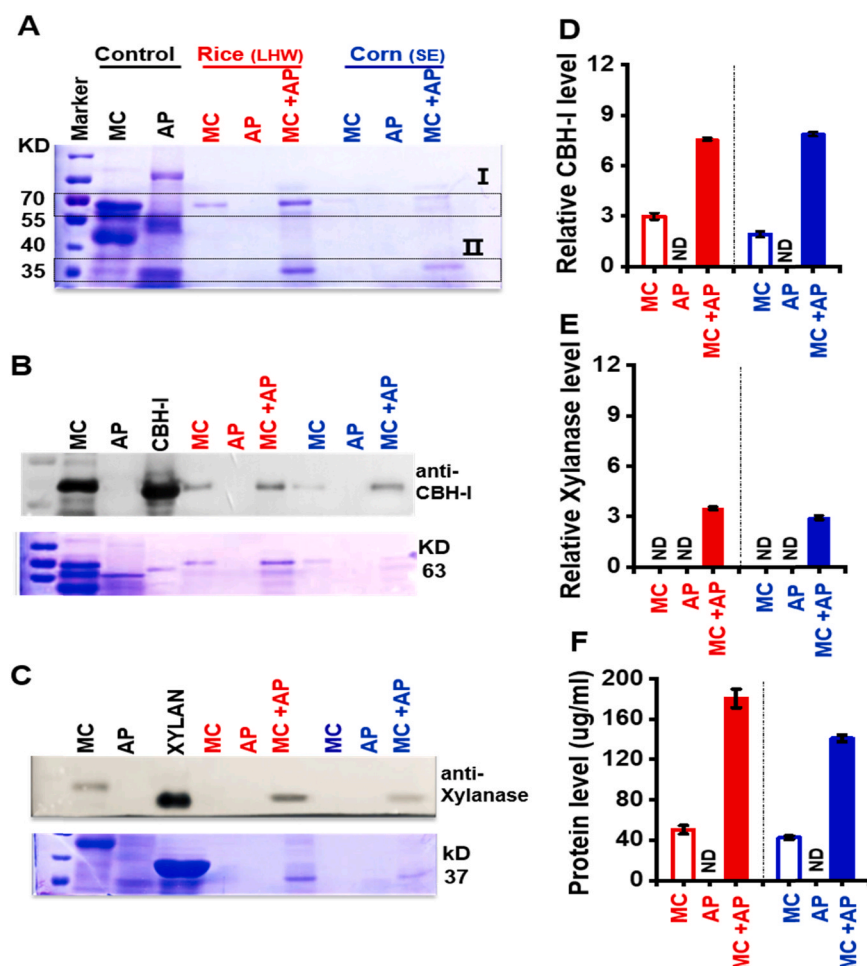


Fig. 4. Detection of *Amaranth* proteins (AP) interaction with lignocellulose residue substrates. (A, B, C) SDS-PAGE and Western blot analyses of soluble proteins collected from the supernatants of mixed-cellulases (MC) hydrolyzes of pretreated rice and corn lignocellulose residues using anti-exo- β -1,4-D-glucanase (CBH-I) and anti-xylanase. AP: *Amaranth* proteins; MC + AP: Mixed-cellulases hydrolysis co-supplied with the AP. (D, E) Measurements of relative levels of CBH-I and xylanase detected in (B) and (C). (F) Total soluble proteins levels detected in (B) and (C). Data as means \pm SD (n = 3).

biomass yield (Table S4) and a complete biomass enzymatic saccharification with 8% *Amaranth* proteins achieved in this study, the *Amaranth* straw could produce 9.13 tons of bioethanol from per hectare (ha) dry matter /per year, which is 2–4 folds higher than those of other seven bioenergy crops (Fig. S3B). Meanwhile, while co-supplied with 12% soybean proteins, all eight bioenergy crops produced much less bioethanol yields relative to the 8% *Amaranth* proteins, mainly due to the soybean proteins that are of significantly less enhancements on biomass enzymatic saccharification and sugar-ethanol conversion rates. Furthermore, based on the maximum dry biomass yield (54 t/ha/per year) and average proteins (20% dry matter) extracted from the *Amaranth* plant, this study evaluated that the *Amaranth* plant could produce about 11 tons of extractable proteins per hectare, which could be co-supplied to enhance enzymatic hydrolysis of almost 137,500 tons of dry biomass for bioethanol production. In terms of this estimation, we calculated that total *Amaranth* proteins extracted from the *Amaranth* plants grown one-hectare land could be supplied to produce the additional bioethanol yields from 6400 (rapeseeds) to 12,400 tons (rice), as a comparison with the controls without the *Amaranth* proteins supply in eight crops examined in this study (Fig. S3C). By comparison, the soybean proteins extracted from soybean seeds (per ha land/per year) could only produce extra bioethanol yields at less than 1000 tons, which were more than 10-fold less than those of the *Amaranth* proteins supply. Hence, the *Amaranth* proteins supplement should be a cost-effective and green-like technology applicable for enhancing bioethanol production at large scale.

3.4. *Amaranth* proteins effectively block lignin to release active cellulases for efficient enzymatic saccharification

To sort out why the *Amaranth* proteins could universally enhance enzymatic saccharification of diverse lignocelluloses substrates in all crops and trees examined, this study detected both *Amaranth* proteins and mixed-cellulases enzymes interactions with lignocellulose residues (Fig. 4). Using total soluble proteins collected from the supernatants of the enzymatic hydrolyzes reactions with the pretreated rice (LHW) and corn (SE) residues performed at 50 °C for 48 h, this study presented protein separation profiling, based on the 12% SDS-PAGE gel running (Fig. 4A). As a control without any enzymatic hydrolysis reaction conducted, the standard *Amaranth* proteins and mixed-cellulases enzymes (MC) respectively showed their typical protein bands. While the *Amaranth* proteins were not co-supplied into the mixed-cellulases enzymatic hydrolysis, the pretreated rice sample showed one faint band, and none of the detectable bands was found in the pretreated corn sample, indicating that almost all enzymes of the mixed-cellulases should be strongly associated with the lignocellulose substrates to maintain in the pellet during enzymatic hydrolysis reaction. On the other hand, without the mixed-cellulases addition, both rice and corn samples did not exhibit any detectable protein bands from the *Amaranth* proteins co-supplement, suggesting that the *Amaranth* proteins should be fully interacted with the lignocellulose substrates either. However, while the *Amaranth* proteins were co-supplied into the mixed-cellulases enzymatic hydrolysis reaction as performed for standard enzymatic saccharification, the rice and corn samples showed one strong band and other several detectable bands, which were corresponding for enzymes of the mixed-cellulases based on the molecular sizes on the SDS gel. To

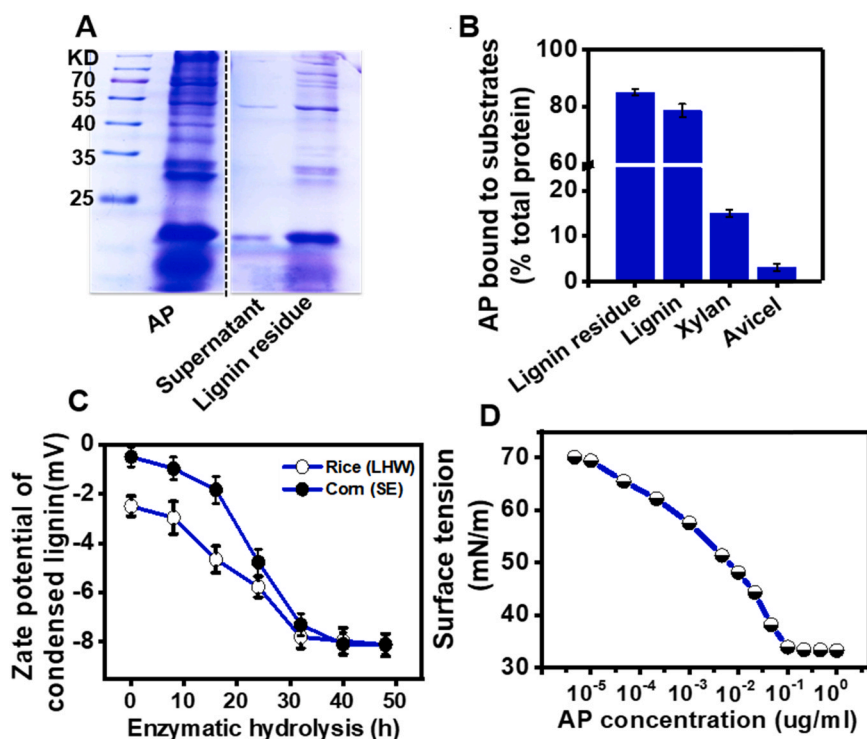


Fig. 5. Characterization of *Amaranth* proteins as bio-surfactant for lignin blocking. (A) SDS-PAGE profiling of proteins distribution in the supernatant and pellet after AP incubation with the rice lignin residue under shaken at 25 °C for 4 h (the rice lignin residue was obtained from complete mixed-cellulases hydrolysis with the pretreated (LHW) rice straw, and washed with distilled water several times until soluble sugars and enzymes were removed). (B) AP binding activities (% of total protein) with the rice lignin residue and three commercial samples (lignin, xylan, and avicel). (C) Zeta potential of lignin microparticles during the time course of mixed-cellulases enzymatic hydrolyzes with pretreated rice (LHW) and corn (SE) residues. (D) Surface tension (mN/m) of AP solutions at a series of concentrations. Data as means \pm SD (n = 3).

test that those bands were derived from the mixed-cellulases, we conducted Western blot analysis using two anti-bodies against exo- β -1,4-D-glucanase (CBH-I) and xylanase, two major enzymes of mixed-cellulases respectively for cellulose and xylan hydrolyzes (Fig. 4B and C). Obviously, both rice and corn samples showed two specific bands of CBH-I and xylanase from supernatants of the mixed-cellulases enzymatic hydrolyzes co-supplied with the *Amaranth* proteins, and those two detectable bands were quantitated to high degrees (Fig. 4D and E), which was confirmed by total protein assay (Fig. 4F). The results thus suggest that the *Amaranth* proteins should effectively block the mixed-cellulases interactions with lignocellulose substrates to release them in the supernatant of the hydrolysis reaction.

3.5. *Amaranth* proteins play a surfactant-like role during lignocellulose enzymatic hydrolysis

To test if the *Amaranth* proteins could act as active biosurfactants for enhancing biomass enzymatic saccharification, this study further performed chemical and biochemical analyses (Fig. 5). Using SDS gel

separation of all molecules of extractable *Amaranth* proteins, we examined that almost all molecules of extractable *Amaranth* proteins could interact with the lignin residue of rice sample in the pellet (Fig. 5A), suggesting that the *Amaranth* proteins should involve in non-specific binding with the lignin residues. This may also explain why the *Amaranth* proteins could play a universal enhancement role for lignocellulose enzymatic saccharification of all major grassy and woody bioenergy crops examined. Based on liquid chromatography electrospray ionization tandem mass spectrometry evaluation, total of 13 distinct *Amaranth* proteins were identified with molecules ranged from 10.4 kDa to 248.3 kDa and pI values from 4.77 to 9.94, and all extractable proteins were predicted to be the enzymes involved in diverse biological processes (Table S5). Hence, compared to the soybean seed proteins, the *Amaranth* proteins consist of quite more different types of enzymes, interpreting why the low dosage of *Amaranth* proteins supplement could even more enhance biomass enzymatic saccharification than those of the soybean proteins.

Using the lignin residue of rice sample and other three commercial standard samples (lignin, xylan, avicel), this study further detected

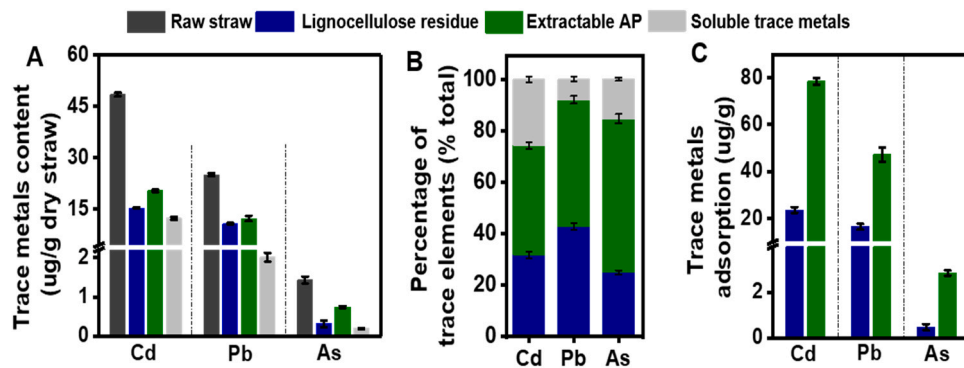


Fig. 6. *Amaranth* proteins (AP) adsorption capacity with trace metals *in vivo*. (A) Cd, Pb, and As contents (ug/g dry straw) in three fractions of *Amaranth* plants grown in land contaminated with trace metals. (B) Proportion of three trace metals detected in (A). (C) Calculation of maximum adsorption capacity (ug/g) *in vivo* of three trace metals in the lignocellulose residue and extractable AP of *Amaranth* straw. Data as means \pm SD (n = 3).

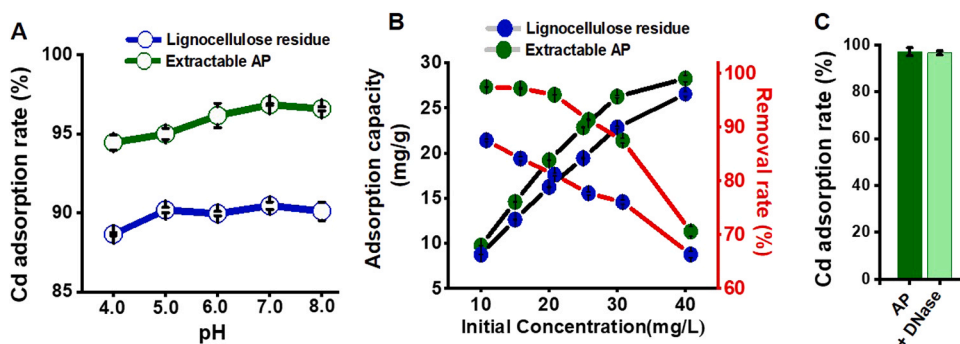


Fig. 7. *Amaranth* proteins (AP) adsorption with trace metals *in vitro*. (A) Cd adsorption rates of lignocellulose residue and extractable AP *in vitro* under different pH values. Incubation time: $C_0 = 2 \text{ mg/L}$, adsorbent dose = 1 g L^{-1} , $T = 25 \pm 2 \text{ }^\circ\text{C}$, $t = 4 \text{ h}$. (B) Cd adsorption capacity and removal rates of lignocellulose residue and extractable AP *in vitro* under initial Cd concentrations, at $\text{pH} = 7.0$ (adsorbent dose = 1 g L^{-1} , $T = 25 \pm 2 \text{ }^\circ\text{C}$, $t = 4 \text{ h}$). (C) Cd adsorption rate of extractable AP without/with DNase. Data as means \pm SD ($n = 3$).

Amaranth proteins binding activity *in vitro* (Fig. 5B). By comparison, the standard lignin sample showed much high binding activity (79%) close to the rice lignin sample (85%), whereas the xylan and avicel samples had extremely low binding activities at 15% and 3%, indicating that lignin molecule was predominately binding with *Amaranth* proteins. Meanwhile, the lignin condensation assay was performed *in vitro*, and the zeta potentials of lignin microparticles were drastically reduced after the mixed-cellulases hydrolyzes were conducted with pretreated rice and corn residues for 30 h (Fig. 5C), which confirmed that lignin could be efficiently binding with the *Amaranth* proteins. In addition, this study detected the surface tension of the *Amaranth* proteins using a standard approach (Zhu et al., 2019). While the *Amaranth* proteins remained raising to supply, they exhibited dynamically reducing surface tension from 70 mN/m to 33.3 mN/m (Fig. 5D), revealing that the *Amaranth* proteins could act like a typical biosurfactant. Taken together, the results have demonstrated that the *Amaranth* proteins could play an effective biosurfactant role for universal enhancements of lignocellulose enzymatic saccharification by non-specifically blocking lignin to maintain free cellulases in all lignocellulose residues examined.

3.6. *Amaranth* proteins are of dominated adsorption capacity with multiple trace metals

As *Amaranthus* plants have been applied for trace metals phytoremediation (Zhou et al., 2016), this study collected the raw straw sample of *Amaranthus* plant grown in the farming land contaminated with multiple trace metals, and then determined high trace metals accumulation in the raw straw such as 45.51 μg cadmium/Cd (per g dry matter), 25.01 μg lead/Pb and 1.43 μg arsenic/As (Fig. 6A). To sort out three trace metals distribution, this study examined three fractions of raw straw: extractable proteins, solid lignocellulose residue, and soluble trace metals. Despite the extractable *Amaranthus* proteins cover 20% of total straw dry weight, they contained the highest contents of three trace metals (20.39 μg Cd, 12.27 μg Pb, 0.74 μg As), respectively covering 43%, 49% and 60% of total trace metals, compared to the lignocellulose residue and soluble metals (Fig. 6A and B). Furthermore, we calculated the extractable *Amaranthus* proteins adsorption capacities ($\mu\text{g/g}$ proteins) with three trace metals such as 78.42 μg Cd, 47.19 μg Pb, and 2.48 μg As, which were 3.3-, 2.9- and 6-folds higher than those of its lignocellulose residue, respectively (Fig. 6C). Therefore, the extractable *Amaranth* proteins should be of dominated adsorption capacity *in vivo* with three trace metals in *Amaranth* straw.

To confirm the *Amaranth* proteins being of the highest adsorption capacity, this study performed a classic Cd^{2+} adsorption analysis *in vitro* using our recently-established approaches (Xu et al., 2020; Zhang et al., 2020). Incubated with Cd^{2+} *in vitro* under a wide range of pH values from 4.0 to 8.0, the *Amaranth* proteins showed much higher Cd^{2+} adsorption rates (%) than those of the *Amaranth* lignocellulose residues (Fig. 7A), consistent with their distinct Cd^{2+} adsorption *in vivo* (Fig. 6C). In particular, the *Amaranth* proteins were of the maximum Cd^{2+} adsorption rate of 97% at pH 7, whereas the lignocellulose residues had

Table 1
Estimation of maximum trace metal accumulation levels (g/ha/year) in plants.

Sample	Trace metal accumulation level (g/ha/year)			References
	Cd	Pb	As	
<i>Amaranth</i>	485	250	14.3	This study
Rice	7.1	20.5	9.3	(Liu et al., 2007)
Wheat	82.8	189	9.1	(Cheng et al., 2019; Liu et al., 2009)
Barley	28	4.2	NA	(Baghaie and Aghili, 2019)
Rapeseed	135	13.7	8.1	(Wu et al., 2019b; Yuan et al., 2020; Zhong et al., 2011)
<i>Miscanthus</i>	51.2	75	6.7	(Cheng et al., 2018; Kocóń and Jurga, 2017)
Sorghum	387	58.8	NA	(Liu et al., 2020; Silas, 2017)
Corn	18.6	88.7	34	(Cao et al., 2019; Chi et al., 2017)
<i>Solanum nigrum</i>	159	55	NA	(Li et al., 2019)
<i>Sedum alfredii</i>	132	NA	NA	(Sun et al., 2014)
<i>Sida hermaphrodita</i>	4	56	NA	(Kocóń and Jurga, 2017)
<i>Noccaea caerulea</i>	130	NA	NA	(Liu et al., 2020)

NA: not available.

the highest adsorption rate of 90%. As the incubation dosage of Cd was raising from 10 mg/L to 40 mg/L, the *Amaranth* proteins remained significantly higher Cd^{2+} adsorption capacities and removal rates, compared to the lignocellulose residues (Fig. 7B). Notably, incubated with the dosage of 40 Cd mg/L, the *Amaranth* proteins were of almost 100% Cd^{2+} removal rate, whereas the lignocellulose residue had the Cd^{2+} removal rate of 95%. In addition, this study examined that the nucleic acids co-extracted with the *Amaranth* proteins did not significantly affect the Cd^{2+} adsorption capacity (Fig. 7C). Therefore, the data of obtained *in vivo* and *in vitro* have demonstrated that the *Amaranth* proteins play a dominated role in trace metals phytoremediation.

In addition, based on the data obtained in this work and previous studies (Table 1), this study briefly estimated the maximum accumulation capacities (g/ha/year) of three major trace metals in the *Amaranthus* plant and other major crops and specific plants examined. As a comparison, the *Amaranthus* plant could accumulate three trace metals at the highest amounts such as 485 Cd, 250 Pb and 14.30 As (g/ha/year), mainly due to its higher biomass yield and trace metal adsorption capacity.

3.7. *Amaranth* proteins are involved in multiple chemical interlinkages with Cd

With respect to the *Amaranth* proteins being of the higher Cd^{2+} adsorption capacity *in vitro*, this study detected their potential chemical interlinkages with the Cd^{2+} using X-ray photoelectron spectroscopy (XPS) (Yu et al., 2008). Compared to the control without Cd^{2+} , the extractable *Amaranth* proteins obviously exhibited two additional peaks

Table 2
Identification of chemical bonds in extractable *Amaranth* proteins by XPS assay.

Sample	Area ration (%)					
	NH ₂ /C=N	C-C/C-H	C-O	O=C-O	C=O	OH
Extractable AP	100	69.84	76.91	13.25	27.20	72.80
Extractable AP + Cd	81.49	49.60	28.65	21.75	52.43	47.57

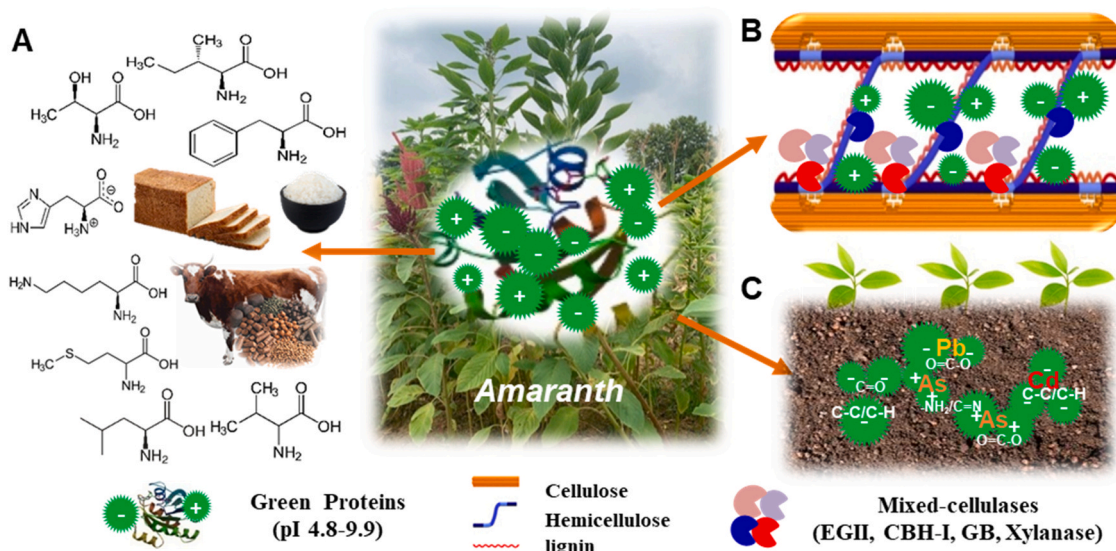


Fig. 8. A hypothetical model highlighting why the *Amaranth* proteins are applicable as high quality of proteins additives into food and feed and universal biosurfactant and biosorbent for enhanced lignocellulose enzymatic saccharification and trace metal remediation.

from their incubation with the Cd²⁺ *in vitro* (Fig. S4A). The appeared peaks in the spectrum of 412.5 eV and 406 eV have been previously characterized as 3d (Cd) and Cd-O linkages, suggesting that the *Amaranth* proteins should be interlinked with Cd²⁺ by chemical bonds (Xu et al., 2020). Meanwhile, this study observed the N 1s, C 1s and O 1s peaks corresponding for nitrogen, carbon and oxygen spectra, and detected obviously shifted peaks in the *Amaranth* proteins sample incubated with Cd²⁺ *in vitro*, relative to the control without Cd²⁺, revealing that six chemical bonds (–NH₂/C=N, C–C/C–H, C–O, O=C–O, C=O, –OH) may all involve in the *Amaranth* proteins adsorption with Cd²⁺ (Fig. S4B–F; Table 2). This may interpret that the *Amaranth* proteins were of much high adsorption capacity with trace metals, due to many different types of *Amaranth* proteins that provided multiple chemical interlinkages with trace metals.

3.8. Mechanisms of the universal enhancements of *Amaranth* proteins for lignocellulose enzymatic saccharification and trace metal remediation

To understand why the *Amaranth* proteins could play universal enhancement roles in lignocellulose enzymatic saccharification and trace metal remediation, we proposed a mechanism model using the data obtained in this work and reported in the previous studies (Fig. 8). Because the *Amaranth* green tissues contain more than ten distinct proteins/enzymes involved in diverse biological processes with molecules ranged from 10.4 kDa to 248.3 kDa and pI values from 4.77 to 9.94, the extractable proteins could provide all eight human-essential amino acids at high levels compared to other green proteins (Carrera et al., 2011; Gorinstein et al., 2002), which should be thus applicable for the high quality of proteins additives into food and feed (Fig. 8A). As almost all types of green proteins could be precipitated with lignocellulose residues to release active mixed-cellulases by mainly interlinking

with lignin (Fig. 8B), it should explain why the green proteins at low dosages could much more enhance the enzymatic saccharification of all distinct lignocellulose residues generated from various physical and chemical pretreatments examined in eight major grassy and woody plants, compared to the soybean seed proteins containing much less types of proteins (Florencio et al., 2016; Luo et al., 2019). It also suggests that all types of lignin molecules in pretreated lignocellulose residues should be well blocked by the green proteins, leading to the mixed-cellulases releases for efficient lignocellulose enzymatic hydrolyzes. Meanwhile, it is also understandable that the green proteins cause much more enhancements to all lignocellulose enzymatic hydrolyzes than those of the classic chemical surfactant Tween-80, mainly due to the diverse molecular sizes and biochemical properties of the green proteins enabled to block any types of pretreated lignocellulose residues. Furthermore, the green proteins are of largely varied pI values and chemical groups, which should be the major factors accounting for their high accumulation *in vivo* with multiple trace metals (Cd, Pb, As) examined in this study (Fig. 8C). In addition, the model highlights that the green proteins should enable to act as a dominated biosorbent with trace metals *via* various chemical bonds *in vitro*. Therefore, the chemical and biochemical diversities of green proteins have determined a wide range of applications such as the excellent nutrition additives into food and feed, the universal biosurfactant into lignocellulose enzymatic degradation for biofuels and other biochemical production and the dominated biosorbent for trace metal remediation.

4. Conclusion

This study characterized the more than 20% extractable green proteins of *Amaranthus retroflexus* L. plants consisting of diverse biological process enzymes, which dually act as universal biosurfactant and

dominated biosorbent respectively for cost-effective lignocellulose enzymatic saccharification and green-like trace metal remediation at large scale. Based on integrated protein profiling and chemical analysis, this study further demonstrated that the extractable green proteins could either effectively block lignin to release active cellulases for enhancing enzymatic degradation of all distinct lignocellulose substrates examined in eight grassy and woody plants or interact with multiple trace metals via various chemical bonds for rising trace metal adsorption capacity. Hence, this study has proposed a novel strategy not only for low-costly lignocellulose utilization of all crop straws and tree residues, but also for high-efficient trace metal remediation of polluted farming lands under a green-like manner.

CRedit authorship contribution statement

Meysam Madadi: Investigation, Methodology, Formal analysis, Writing - original draft. **Youmei Wang:** Methodology, Formal analysis, Validation. **Chengbao Xu:** Methodology, Formal analysis. **Peng Liu:** Methodology, Formal analysis. **Yanting Wang:** Validation, Project administration. **Tao Xia:** Editing, Validation. **Yuanyuan Tu:** Formal analysis, Methodology. **Xinchun Li:** Formal analysis, Methodology. **Bo Song:** Resources. **Xiaoe Yang:** Methodology, Investigation. **Wanbin Zhu:** Methodology, Investigation. **Deqiang Duanmu:** Editing, Project administration. **Shang-wen Tang:** Conceptualization, Co-supervision, Funding acquisition. **Liangcai Peng:** Conceptualization, Writing - original draft, Writing - review & editing, Supervision, Funding acquisition.

Declaration of Competing Interest

The authors declare that they have no known competing financial interests or personal relationships that could have appeared to influence the work reported in this paper.

Acknowledgments

We thank that the China Amaranth Ecological Technology Co., Ltd. kindly provided the experimental materials of Amaranth retroflexus L. plants. This study supported by the projects of Huazhong Agricultural University Independent Scientific & Technological Innovation Foundation (2662020ZKPY013; 2662019PY054), the National Natural Science Foundation of China (32000381), the National Key Research and Development Program of China (2016YFD0800804), the National 111 Project of Ministry of Education of China (BP0820035), and the Project of Hubei University of Arts and Science (XKQ2018006).

Appendix A. Supplementary material

Supplementary data associated with this article can be found in the online version at [doi:10.1016/j.jhazmat.2020.124727](https://doi.org/10.1016/j.jhazmat.2020.124727).

References

- Akond, M., Islam, S., Wang, X., 2013. Characterization of biomass traits and cell wall components among diverse accession of Amaranthaceae. *J. Appl. Phytotechnol. Environ. Sanit.* 2, 37–45.
- Alam, A., Zhang, R., Liu, P., Huang, J., Wang, Y., Hu, Z., Madadi, M., Sun, D., Hu, R., Ragauskas, A.J., Tu, Y., Peng, L., 2019. A finalized determinant for complete lignocellulose enzymatic saccharification potential to maximize bioethanol production in bioenergy *Miscanthus*. *Biotechnol. Biofuels* 12, 99.
- Andini, R., Yoshida, S., Ohsawa, R., 2013. Variation in protein content and amino acids in the leaves of grain, vegetable and weedy types of *Amaranthus*. *Agronomy* 3, 391–403.
- Baghaie, A.H., Aghili, F., 2019. Health risk assessment of Pb and Cd in soil, wheat, and barley in Shazand County, Central of Iran. *J. Environ. Health Sci. Eng.* 17, 467–477.
- Baruah, J., Nath, B.K., Sharma, R., Kumar, S., Deka, R.C., Baruah, D.C., Kalita, E., 2018. Recent trends in the pretreatment of lignocellulosic biomass for value-added products. *Front. Energy Res.* 6, 141.

- Brondi, M.G., Vasconcellos, V.M., Giordano, R.C., Farinas, C.S., 2019. Alternative low-cost additives to improve the saccharification of lignocellulosic biomass. *Appl. Biochem. Biotechnol.* 187, 461–473.
- Cao, X., Bai, L., Zeng, X., Zhang, J., Wang, Y., Wu, C., Su, S., 2019. Is maize suitable for substitution planting in arsenic-contaminated farmlands? *Plant Soil Environ.* 65, 425–434.
- Carrera, C.S., Reynoso, C.M., Funes, G.J., Martínez, M.J., Dardanelli, J., Resnik, S.L., 2011. Amino acid composition of soybean seeds as affected by climatic variables. *Pesqui. Agropecu. Bras.* 46, 1579–1587.
- Chen, X., Kuhn, E., Jennings, E.W., Nelson, R., Tao, L., Zhang, M., Tucker, M.P., 2016. DMR (deacetylation and mechanical refining) processing of corn stover achieves high monomeric sugar concentrations (230 g L⁻¹) during enzymatic hydrolysis and high ethanol concentrations (>10% v/v) during fermentation without hydrolysate purification or concentration. *Energy Environ. Sci.* 9, 1237–1245.
- Cheng, L., Wang, L., Wei, L., Wu, Y., Alam, A., Xu, C., Wang, Y., Tu, Y., Peng, L., Xia, T., 2019. Combined mild chemical pretreatments for complete cadmium release and cellulosic ethanol co-production distinctive in wheat mutant straw. *Green Chem.* 21, 3693–3700.
- Cheng, S., Yu, H., Hu, M., Wu, Y., Cheng, L., Cai, Q., Tu, Y., Xia, T., Peng, L., 2018. *Miscanthus* accessions distinctively accumulate cadmium for largely enhanced biomass enzymatic saccharification by increasing hemicellulose and pectin and reducing cellulose CrI and DP. *Bioresour. Technol.* 263, 67–74.
- Chi, T., Zuo, J., Liu, F., 2017. Performance and mechanism for cadmium and lead adsorption from water and soil by corn straw biochar. *Front. Environ. Sci. Eng.* 11, 15.
- Da Silva, T.E., Detmann, E., Franco, M.D.O., Palma, M.N.N., Rocha, G.C., 2016. Evaluation of digestion procedures in Kjeldahl method to quantify total nitrogen in analyses applied to animal nutrition. *Acta Sci. Anim. Sci.* 38, 45–51.
- De Souza, R.O.M.A., Miranda, L.S.M., Luque, R., 2014. Bio(chemo)technological strategies for biomass conversion into bioethanol and key carboxylic acids. *Green Chem.* 16, 2386–2405.
- Demartini, J.D., Pattathil, S., Miller, J.S., Li, H., Hahn, M.G., Wyman, C.E., 2013. Investigating plant cell wall components that affect biomass recalcitrance in poplar and switchgrass. *Energy Environ. Sci.* 6, 898–909.
- Deng, J., Zhu, X., Chen, P., He, B., Tang, S.W., Zhao, W., Li, X., Zhang, R., Lv, Z., Kang, H., Yu, L., Peng, L., 2020. Mechanism of lignocellulose modification and enzyme disadsorption for complete biomass saccharification to maximize bioethanol yield in rapeseed stalks. *Sustain. Energy Fuels* 4, 607–618.
- Dische, Z., Pallavicini, C., Kawasaki, H., Smirnov, N., Cizek, L.J., Chien, S., 1962. Influence of the nature of the secretory stimulus on the composition of the carbohydrate moiety of glycoproteins of the submaxillary saliva. *Arch. Biochem. Biophys.* 97, 459–469.
- Dos Santos, A.C., Ximenes, E., Kim, Y., Ladisch, M.R., 2019. Lignin-enzyme interactions in the hydrolysis of lignocellulosic biomass. *Trends Biotechnol.* 37, 518–531.
- Florencio, C., Badino, A.C., Farinas, C.S., 2016. Soybean protein as a cost-effective lignin-blocking additive for the saccharification of sugarcane bagasse. *Bioresour. Technol.* 221, 172–180.
- Fry, S.C., 2000. *The Growing Plant Cell Wall: Chemical and Metabolic Analysis*. Longman, London.
- Gorinstein, S., Pawelzik, E., Delgado-Licon, E., Haruenkit, R., Weisz, M., Traktenberg, S., 2002. Characterisation of pseudocereal and cereal proteins by protein and amino acid analyses. *J. Sci. Food Agric.* 82, 886–891.
- Grobelnik Malakar, S., Turinek, M., Jakop, M., Bavec, M., Bavec, F., 2010. Grain *Amaranth* as an alternative and perspective crop in temperate climate. *J. Geogr.* 5, 135–145.
- Henshaw, J.L., Bolam, D.N., Pires, V.M.R., Czjzek, M., Henrissat, B., Ferreira, L.M.A., Fontes, C.M.G.A., Gilbert, H.J., 2004. The family 6 carbohydrate binding module CmCBM6-2 contains two ligand-binding sites with distinct specificities. *J. Biol. Chem.* 279, 21552–21559.
- Hu, M., Yu, H., Li, Y., Li, A., Cai, Q., Liu, P., Tu, Y., Wang, Y., Hu, R., Hao, B., Peng, L., Xia, T., 2018. Distinct polymer extraction and cellulose DP reduction for complete cellulose hydrolysis under mild chemical pretreatments in sugarcane. *Carbohydr. Polym.* 202, 434–443.
- Jin, W., Chen, L., Hu, M., Sun, D., Li, A., Li, Ying, Hu, Z., Zhou, S., Tu, Y., Xia, T., Wang, Y., Xie, G., Li, Yanbin, Bai, B., Peng, L., 2016. Tween-80 is effective for enhancing steam-exploded biomass enzymatic saccharification and ethanol production by specifically lessening cellulase absorption with lignin in common reed. *Appl. Energy* 175, 82–90.
- Jonathan, Tucker, 1986. *Amaranth: The Once and Future Crop*, 36. Oxford University Press, pp. 9–13.
- Kim, Y., Thomas, A.E., Robichaud, D.J., Lisa St., K., John, P.C., Etz, B.D., Fioroni, G.M., Dutta, A., McCormick, R.L., Mukarakate, C., Kim, S., 2020. A perspective on biomass-derived biofuels: from catalyst design principles to fuel properties. *J. Hazard. Mater.* 400, 123198.
- Kocoi, A., Jurga, B., 2017. The evaluation of growth and phytoextraction potential of *Miscanthus × giganteus* and *Sida hermaphrodita* on soil contaminated simultaneously with Cd, Cu, Ni, Pb, and Zn. *Environ. Sci. Pollut. Res.* 24, 4990–5000.
- Li, F., Xie, G., Huang, J., Zhang, R., Li, Y., Zhang, M., Wang, Y., Li, A., Li, X., Xia, T., Qu, C., Hu, F., Ragauskas, A.J., Peng, L., 2017. OsCESA9 conserved-site mutation leads to largely enhanced plant lodging resistance and biomass enzymatic saccharification by reducing cellulose DP and crystallinity in rice. *Plant Biotechnol. J.* 15, 1093–1104.
- Li, F., Zhang, M., Guo, K., Hu, Z., Zhang, R., Feng, Y., Yi, X., Zou, W., Wang, L., Wu, C., Tian, J., Lu, T., Xie, G., Peng, L., 2015. High-level hemicellulosic arabinose predominately affects lignocellulose crystallinity for genetically enhancing both plant lodging resistance and biomass enzymatic digestibility in rice mutants. *Plant Biotechnol. J.* 13, 514–525.

- Li, X., Zhang, X., Wang, X., Cui, Z., 2019. Phytoremediation of multi-metal contaminated mine tailings with *Solanum nigrum* L. and biochar/attapulgite amendments. *Ecotoxicol. Environ. Saf.* 180, 517–525.
- Li, Y., Liu, P., Huang, J., Zhang, R., Hu, Z., Peng, S., Wang, Y., Wang, L., Xia, T., Peng, L., 2018. Mild chemical pretreatments are sufficient for bioethanol production in transgenic rice straws overproducing glucosidase. *Green Chem.* 20, 2047–2056.
- Liu, C., Xiao, Y., Xia, X., Zhao, X., Peng, L., Srinophakun, P., 2018. Cellulosic ethanol production: progress, challenges and strategies for solutions. *Biotechnol. Adv.* 491–504.
- Liu, W.X., Liu, J.W., Wu, M.Z., Li, Y., Zhao, Y., Li, S.R., 2009. Accumulation and translocation of toxic heavy metals in winter wheat (*Triticum aestivum* L.) growing in agricultural soil of Zhengzhou, China. *Bull. Environ. Contam. Toxicol.* 82, 343–347.
- Liu, W.X., Shen, L.F., Liu, J.W., Wang, Y.W., Li, S.R., 2007. Uptake of toxic heavy metals by rice (*Oryza sativa* L.) cultivated in the agricultural soil near Zhengzhou City, People's Republic of China. *Bull. Environ. Contam. Toxicol.* 79, 209–213.
- Liu, Y., Nie, Y., Lu, X., Zhang, X., He, H., Pan, F., Zhou, L., Liu, X., Ji, X., Zhang, S., 2019. Cascade utilization of lignocellulosic biomass to high-value products. *Green Chem.* 21, 3499–3535.
- Liu, Z.Q., Li, H.L., Zeng, X.J., Lu, C., Fu, J.Y., Guo, L.J., Kimani, W.M., Yan, H.L., He, Z.Y., Hao, H.Q., Jing, H.C., 2020. Coupling phytoremediation of cadmium-contaminated soil with safe crop production based on a sorghum farming system. *J. Clean. Prod.* 275, 123002.
- Luo, X., Liu, J., Zheng, P., Li, M., Zhou, Y., Huang, L., Chen, L., Shuai, L., 2019. Promoting enzymatic hydrolysis of lignocellulosic biomass by inexpensive soy protein. *Biotechnol. Biofuels* 12, 51.
- Mariotti, F., Tomé, D., Mirand, P.P., 2008. Converting nitrogen into protein – beyond 6.25 and Jones' factors. *Crit. Rev. Food Sci. Nutr.* 48, 177–184.
- Peng, J., feng, Song, Y. hui, Yuan, P., Cui, X. yu, Qiu, G. lei, 2009. The remediation of heavy metals contaminated sediment. *J. Hazard. Mater.* 161, 633–640.
- Peng, L., Hocart, C.H., Redmond, J.W., Williamson, R.E., 2000. Fractionation of carbohydrates in *Arabidopsis* root cell walls shows that three radial swelling loci are specifically involved in cellulose production. *Planta* 211, 406–414.
- Ragauskas, A.J., Williams, C.K., Davison, B.H., Britovsek, G., Cairney, J., Eckert Jr., C.A., Hallett, W.J.F., Leak, J.P., Liotta, D.J., Mielenz, C.L., Murphy, J.R., Templar, R., Tschaplinski, T. R., 2006. The path forward for biofuels. *Science* 311, 484–489.
- Shinde, S.D., Meng, X., Kumar, R., Ragauskas, A.J., 2018. Recent advances in understanding the pseudo-lignin formation in a lignocellulosic biorefinery. *Green Chem.* 20, 2192–2205.
- Silas, T.V., 2017. Characterization and adsorption isotherm studies of Cd (II) And Pb (II) ions bioremediation from aqueous solution using unmodified sorghum husk. *JABB* 2, 00034.
- Sluiter, A., Hames, B., Ruiz, R., Scarlata, C., Slui, J., Templeton, D., Crocker, D., 2008. Determination of structural carbohydrates and lignin in biomass. *Lab. Anal. Proced.* 1617, 1–16.
- Sun, D., Alam, A., Tu, Y., Zhou, S., Wang, Y., Xia, T., Huang, J., Li, Y., Zahoor, Wei, X., Hao, B., Peng, L., 2017. Steam-exploded biomass saccharification is predominately affected by lignocellulose porosity and largely enhanced by Tween-80 in *Miscanthus*. *Bioresour. Technol.* 239, 74–81.
- Sun, D., Yang, Q., Wang, Yanting, Gao, H., He, M., Lin, X., Lu, J., Wang, Youmei, Kang, H., Alam, A., Tu, Y., Xia, T., Peng, L., 2020. Distinct mechanisms of enzymatic saccharification and bioethanol conversion enhancement by three surfactants under steam explosion and mild chemical pretreatments in bioenergy *Miscanthus*. *Ind. Crops Prod.* 153, 112559.
- Sun, J., Murthy Konda, N.V.S.N., Shi, J., Parthasarathi, R., Dutta, T., Xu, F., Scown, C.D., Simmons, B.A., Singh, S., 2016. CO₂ enabled process integration for the production of cellulosic ethanol using bionic liquids. *Energy Environ. Sci.* 9, 2822–2834.
- Sun, Y., Wu, Q.T., Lee, C.C.C., Li, B., Long, X., 2014. Cadmium sorption characteristics of soil amendments and its relationship with the cadmium uptake by hyperaccumulator and normal plants in amended soils. *Int. J. Phytoremediat.* 16, 496–508.
- Vardhan, K.H., Kumar, P.S., Panda, R.C., 2019. A review on heavy metal pollution, toxicity and remedial measures: current trends and future perspectives. *J. Mol. Liq.* 290, 111197.
- Viglasky, J., Andrejack, I., Huska, J., Suchomel, J., 2009. *Amaranth* (*Amarantus* L.) is a potential source of raw material for biofuels production. *Agron. Res.* 7, 865–873.
- Wang, W., Zhuang, X., Tan, X., Wang, Q., Chen, X., Yu, Q., Qi, W., Wang, Z., Yuan, Z., 2018. Dual effect of nonionic surfactants on improving the enzymatic hydrolysis of lignocellulose. *Energy Fuels* 32, 5951–5959.
- Wang, Y., Fan, C., Hu, H., Li, Y., Sun, D., Wang, Youmei, Peng, L., 2016. Genetic modification of plant cell walls to enhance biomass yield and biofuel production in bioenergy crops. *Biotechnol. Adv.* 34, 997–1017.
- Wei, W., Wu, S., 2017. Enhanced enzymatic hydrolysis of eucalyptus by synergy of zinc chloride hydrate pretreatment and bovine serum albumin. *Bioresour. Technol.* 245, 289–295.
- Wu, L., Feng, S., Deng, J., Yu, B., Wang, Y., He, B., Peng, H., Li, Q., Hu, R., Peng, L., 2019a. Altered carbon assimilation and cellulose accessibility to maximize bioethanol yield under low-cost biomass processing in corn brittle stalk. *Green Chem.* 21, 4388–4399.
- Wu, Y., Wang, M., Yu, L., Tang, S., Xia, T., Kang, H., Xu, C., Gao, H., Madadi, M., Alam, A., Cheng, L., Peng, L., 2019b. A mechanism for efficient cadmium phytoremediation and high bioethanol production by combined mild chemical pretreatments with desirable rapeseed stalks. *Sci. Total Environ.* 708, 135096.
- Xu, C., Xia, T., Wang, J., Yu, L., Wu, L., Zhang, Y., Liu, P., Chen, P., Peng, S., Peng, L., 2020. Selectively desirable rapeseed and corn stalks distinctive for low-cost bioethanol production and high-active biosorbents. *Waste Biomass Valoriz.* <https://doi.org/10.1007/s12649-020-01026-0>.
- Yang, Y., Tilman, D., Lehman, C., Trost, J.J., 2018. Sustainable intensification of high-diversity biomass production for optimal biofuel benefits. *Nat. Sustain.* 1, 686–692.
- Yu, J., Tong, M., Sun, X., Li, B., 2008. Enhanced and selective adsorption of Pb²⁺ and Cu²⁺ by EDTAD-modified biomass of baker's yeast. *Bioresour. Technol.* 99, 2588–2593.
- Yu, J.X., Wang, L.Y., Chi, R.A., Zhang, Y.F., Xu, Z.G., Guo, J., 2015. Adsorption of Pb²⁺, Cd²⁺, Cu²⁺, and Zn²⁺ from aqueous solution by modified sugarcane bagasse. *Res. Chem. Intermed.* 41, 1525–1541.
- Yuan, T., Gu, J., Zhou, H., Huang, F., Yang, W., Wang, S., Zhang, J., Huo, Y., Liao, B., 2020. Translocation and accumulation of cadmium and lead in the tissues of 39 rape cultivars grown in a polluted farmland. *Environ. Sci. Pollut. Res.* 27, 15888–15900.
- Zahoor, Sun, D., Li, Y., Wang, J., Tu, Y., Wang, Y., Hu, Z., Zhou, S., Wang, L., Xie, G., Huang, J., Alam, A., Peng, L., 2017. Biomass saccharification is largely enhanced by altering wall polymer features and reducing silicon accumulation in rice cultivars harvested from nitrogen fertilizer supply. *Bioresour. Technol.* 243, 957–965.
- Zhang, Y., Xu, C., Lu, J., Yu, H., Zhu, J., Zhou, J., Zhang, X., Liu, F., Wang, Y., Hao, B., Peng, L., Xia, T., 2020. An effective strategy for dual enhancements on bioethanol production and trace metal removal using *Miscanthus* straws. *Ind. Crops Prod.* 152, 112393.
- Zhong, L., Hu, C., Tan, Q., Liu, J., Sun, X., 2011. Effects of sulfur application on sulfur and arsenic absorption by rapeseed in arsenic-contaminated soil. *Plant Soil Environ.* 57, 429–434.
- Zhou, H., Yang, W.T., Zhou, X., Liu, L., Gu, J.F., Wang, W.L., Zou, J.L., Tian, T., Peng, P. Q., Liao, B.H., 2016. Accumulation of heavy metals in vegetable species planted in contaminated soils and the health risk assessment. *IJERPH* 13, 289.
- Zhou, X., Li, Q., Zhang, Y., Gu, Y., 2017. Effect of hydrothermal pretreatment on *Miscanthus* anaerobic digestion. *Bioresour. Technol.* 224, 721–726.
- Zhou, Y., Chen, H., Qi, F., Zhao, X., Liu, D., 2015. Non-ionic surfactants do not consistently improve the enzymatic hydrolysis of pure cellulose. *Bioresour. Technol.* 182, 136–143.
- Zhu, F., Cao, C., Cao, L., Li, F., Du, F., Huang, Q., 2019. Wetting behavior and maximum retention of aqueous surfactant solutions on tea leaves. *Molecules* 24, 2094.